NACA TN 3380

NATIONAL ADVISORY COMMITTEE FOR AERONAUTICS

TECHNICAL NOTE 3380

STUDY OF EFFECTS OF MICROSTRUCTURE AND ANISOTROPY ON FATIGUE OF 24S-T4 ALUMINUM ALLOY

By H. A. Lipsitt, G. E. Dieter,
G. T. Horne, and R. F. Mehl

Carnegie Institute of Technology

Washington
March 1955

NATIONAL ADVISORY COMMITTEE FOR AERONAUTICS

TECHNICAL NOTE 3380

STUDY OF EFFECTS OF MICROSTRUCTURE AND ANISOTROPY ON FATIGUE OF 24S-T4 ALUMINUM ALLOY

By H. A. Lipsitt, G. E. Dieter,
G. T. Horne, and R. F. Mehl

SUMMARY

The present investigation utilized previously developed and reported statistical methods to study the effects of variation in microstructure (extruded and extruded plus recrystallized) on the fatigue properties of 24S-T4 aluminum-alloy notched specimens tested in both the longitudinal and transverse directions.

The results show that a definite anisotropy exists in the fatigue strength of this alloy in these tests. This anisotropy is found only for the material in the extruded condition; the extruded and recrystallized material shows no significant anisotropy and essentially the same fatigue properties as the extruded material in the transverse direction. Correlation tests with unnotched extruded longitudinal specimens showed that there is more scatter in unnotched than in notched specimens; within the range of stresses tested (and of resulting life), the fatigue-strength reduction factor K_f increases with increasing stress. The effect of microstructure on the resulting fractures was also investigated.

INTRODUCTION

The initial investigation of the statistical nature of fatigue properties in this laboratory, in which the endurance limit of steel was shown to be of a statistical nature, was reported by Ransom and Mehl (ref. 1). Following this the fatigue-fracture statistics of steel were shown by Epremian and Mehl (ref. 2) to be most influenced by the nonmetallic inclusions present. Dieter and Mehl (ref. 3) studied the effect of carbide morphology on the fatigue statistics and also the statistical variations present in some commercial aluminum alloys. The most recent contribution of this laboratory, a study of the overstressing phenomenon in SAE 4340 steel, was made by Dieter, Horne, and Mehl (ref. 4).

The purpose of the present investigation was to study further the effects of variation in microstructure and the statistical changes arising from the use of a notch (or stress-raiser). The material, 24S aluminum alloy, was chosen as being one of direct interest in aircraft construction. Information on the fatigue properties of 24S aluminum alloy with two different microstructures (grains elongated by extrusion and more nearly equiaxed grains resulting from recrystallization following extrusion) is of great interest to the aircraft industry, where such a condition is a very real problem. Many aluminum extrusions, such as wing spars, show a recrystallized layer upon heat-treating after extrusion and it would be desirable to know how the dual microstructure affects the fatigue properties of the construction material. Such "composite" structures have not, of course, been tested here, but the components have, in the hope that the composite behaves as the sum of its components. It was known that the tensile properties were lower for the recrystallized material, but little information was available on the fatigue properties under these conditions.

The problem was chosen, then, because of its immediate industrial interest and also because it would serve to provide further information on the statistical nature of fatigue, particularly on the effects of variation in microstructure and on the effects of a mild stress concentration provided by a notch. A notch with a theoretical stress-concentration factor K_t of 2.25 was used. An additional reason for the use of a notch was to check the failure theory of Epremian and Mehl (ref. 2). In light of this theory the probability of failure would be lower for a specimen where the location of failure is constrained by a notch. Hence, greater statistical scatter would be expected. On the other hand, the stress concentration and high stress gradient produced by the notch would correspond to the "high-stress" condition of the previous theory, and hence the use of a notch would lead to smaller statistical scatter. A correlation with unnotched specimens of the same material would show which of these tendencies predominated in influencing the scatter in fatigue life.

All statistical tests on data from this investigation were run at the 95-percent confidence level (the 5-percent level of significance).

This investigation was conducted at Carnegie Institute of Technology under the sponsorship and with the financial assistance of the National Advisory Committee for Aeronautics. The authors would like to acknowledge the invaluable assistance of Mr. J. P. Bucci in many phases of this work.

SYMBOLS AND NOMENCLATURE

K_f	fatigue-strength reduction factor
K_t	theoretical stress-concentration factor

N	number of cycles to failure for a given specimen
$\log N$	common logarithm of N
$\overline{\log N}$	arithmetic mean of $\log N$ for n specimens; unbiased estimate of mean of universe of $\log N$, $\sum_{i=1}^{i=n} \frac{\log N_i}{n}$
$\overline{N}$	antilogarithm of $\overline{\log N}$; median of universe of N when $\log N$ is normally distributed
n	sample size; number of specimens tested at stress S
S	maximum value of alternating stress (mean stress in this investigation was zero)
σ	unbiased estimate of standard deviation of universe of $\log N$, $\sigma_n\left(\frac{n}{n-1}\right)^{1/2}$
$\sigma_{\overline{\log N}}$	standard error of $\overline{\log N}$, $\sigma/\sqrt{n}$
σ_n	standard deviation of $\log N$ obtained from sample of n observations, $\left[\frac{\sum_{i=1}^{i=n}(\log N_i)^2}{n} - (\overline{\log N})^2\right]^{1/2}$
S.D.	statistically significant difference exists between quantities compared at chosen level of confidence
N.S.D.	no statistically significant difference exists between quantities compared at chosen level of confidence
EL	extruded longitudinal; specimens of extruded material with fiber (extrusion) direction parallel to specimen axis
ET	extruded transverse; specimens of extruded material with fiber (extrusion) direction perpendicular to specimen axis
RL	recrystallized longitudinal; specimens of recrystallized material with specimen axis parallel to extrusion direction

RT recrystallized transverse; specimens of recrystallized material with specimen axis perpendicular to extrusion direction

LITERATURE REVIEW

Information on the fatigue statistics of aluminum alloys is limited and a review of most of the important literature has been presented by Dieter and Mehl (ref. 3). They review the work of Ravilly (ref. 5), who found that the scatter in aluminum was somewhat less than that for similar specimens of annealed steel and Armco iron. They also review the work of Yen and Dolan (ref. 6) and Dolan and Brown (ref. 7), in which it was shown that the scatter in 75S-T increased generally with decrease in stress and also that the curve of S versus $\overline{\log N}$ was concave upward.

In order to employ simple tests of significance in studies of this nature, it is necessary to assume that the log N values have a normal distribution. Evidence of the approximate validity of this assumption has been found many times in the past and more recently by Head (ref. 8). He studied 24S-T using rotating cantilever tests and again found that the distribution of values of log N was approximately normal.

Templin, Howell, and Hartmann (ref. 9) studied the effect of grain direction on the fatigue properties of 14S, 24S, and 75S employing both notched and smooth specimens. They concluded that the fatigue strengths determined in the transverse direction are not significantly different from those for the longitudinal direction and also that there seems to be a greater spread in fatigue strengths determined on the smooth specimens than in those determined on the notched specimens. The nature of their data did not make it possible to compare the data statistically since the sample size at a given stress was not large enough to calculate reliable statistics.

EXPERIMENTAL WORK

Test Material and Specimen Preparation

All specimens used in this investigation were prepared from material, which was obtained through the courtesy of the Aluminum Company of America. The material was of the following composition:

Material	Composition, percent									
	Cu	Fe	Si	Mn	Mg	Zn	Ni	Cr	Ti	Al
24S	4.66	0.24	0.14	0.70	1.51	0.03	0.01	0.01	0.01	Bal.

The material was fabricated in the following manner: A 1.25-inch by 4-inch by 36-foot bar was extruded from an 11-inch-diameter ingot at a nominal temperature of 800° F and at a speed of 4 feet per minute. Following extrusion the 36-foot piece was cut in half and both halves were straightened by stretching approximately 1.4 percent. The stretched material was then annealed at 775° to 800° F, furnace cooled to 600° F, and air cooled to room temperature. One 18-foot section was further stretched 8.5 percent so that recrystallization would occur upon subsequent heat treatment. Both halves of the extrusion were then given a solution heat treatment at 920° F, according to standard procedure, and quenched in water. The material was then allowed to age naturally at room temperature to a stabilized condition.

X-ray and microscopic examinations at the Aluminum Research Laboratories of the Aluminum Company of America revealed that the material was typical of commercial production. A Laue back-reflection X-ray photogram of the central portion of the extruded material (fig. 1(a)) revealed evidences of extensive deformation. X-ray examination of a central portion of the recrystallized material showed that, while recrystallization had occurred, there still remained evidences of residual deformation (fig. 1(b)).

The bars in both the extruded and the extruded-plus-recrystallized condition show a rim of recrystallized material. The rim on the recrystallized bar stock is merely larger grained than the recrystallized interior and the grains are somewhat more equiaxed. Figure 2(a) shows an end view of the extruded bar. A thin rim of quite large grained material is present. Figure 2(b) shows a top view of the skin of this same bar and it can be seen that the material shows considerable directional properties. It is to be noted that the recrystallized rim covers the entire perimeter of the bar stock and that the specimens shown have been partially cropped; the light outlines in figures 3(b) and 3(c) show the true bar size.

Figure 4(a) shows an end view of the recrystallized bar stock. The very large grained recrystallized rim is thicker than in the extruded bar. The grain size of this rim is shown in figure 4(b), and it may be noted that even with what appears to be complete recrystallization the extrusion direction is unmistakable.

Figures 5(a) to 5(g) show microstructures, unetched and etched, typical of the longitudinal (central region of a section parallel to the 1.25 inch by 36-foot face of the bar, "side" view) and transverse (central region of a section parallel to the 4- by 1.25-inch face of the bar, "end" view) structures. An etched extruded longitudinal microstructure is not shown because of excessive pitting; figures 6(a) and 6(b) show etched macrostructures of extruded and extruded-plus-recrystallized longitudinal sections, respectively, for comparison.

All metallograpic specimens were given an initial mechanical polish followed by a chemical polish in Alcoa R5 Bright Dip. The etchant used, where indicated, was Keller's etch. The unetched specimens show a few grain boundaries due to the action of the chemical polish.

In general, the transverse sections show a nearly random pattern of precipitate with some evidence of agglomeration of precipitate in the recrystallized specimens; the longitudinal sections show a directional distribution of the precipitate. In addition, the recrystallized longitudinal sections show bands clear of precipitate; this was a real phenomenon found throughout this material and the photomicrograph shown is typical.

To secure the specimen blanks the ends were first cropped from the bars and then the bars were cut into sections $3\frac{9}{16}$ inches long as shown in figure 3(a). From the first section of each bar (extruded and extruded plus recrystallized) four longitudinal specimens were taken as shown in figures 3(a) and 3(b). The specimens were numbered with the two outside ones having odd numbers and the two inside ones having even numbers. From the second section of each bar four transverse specimens were cut. The transverse specimen position in the bar stock is shown in figures 3(a) and 3(c). The third section of each bar was used for longitudinal specimens; the fourth, for transverse; and so on throughout the bar length. It may be seen from figures 3(a) to 3(c) that every effort was made to secure specimens having the same microstructure and properties in the notched region.

Each specimen was numbered as indicated to show its position in the original bar stock. In order to eliminate errors that might arise because of slight property variations over the bar length, the specimens were randomized before testing. The procedure was to test the specimens in the order that their bar-position numbers appeared on a table of random numbers. The data, as gathered, were tested statistically to determine if there was any apparent trend of fatigue properties with position; no such trend, in any of the series of tests, was found.

That this material is highly anisotropic is shown (table I) by its mechanical properties. To obtain the tensile properties the first, twentieth, thirty-fifth, fiftieth, and seventieth specimen blanks were used and the results presented in all cases are the average of these five tests. The hardness measurements were made as indicated in table I, and it should be noted here that, as expected, the Brinell impressions were elliptical with a maximum of 0.25-millimeter difference between the major- and minor-axis lengths; the major axis was invariably in the direction of the 4-inch dimension of the stock, perpendicular to the extrusion direction.

TEST EQUIPMENT AND TESTING PROCEDURE

The 24S-T4 aluminum-alloy specimens were tested on four R. R. Moore rotating-beam machines at a nominal speed of 10,000 cpm. The weights were accurately calibrated and the effective dead weight was determined for each machine. The weights were applied with the machine and specimen running at testing speed and the counters immediately reset. The specimens were run to complete fracture in all cases. The minimum diameter of each specimen was measured optically on a comparator (at 20X) to 0.0001 inch.

The applied stress was calculated by the formula

$$S = \frac{Mc}{I} = \frac{16PL}{\pi D^3}$$

where

S	applied stress, psi
M	bending moment, in-lb
c	distance from outermost fiber to neutral axis, in.
I	moment of inertia, $in.^4$
P	total applied load, lb
L	lever-arm length, in.
D	minimum or notch diameter of specimen, in.

The maximum percentage error in stress was about ±0.7 percent. Here, again, the data were analyzed to determine if there was any apparent "machine effect" leading to significant differences of fatigue life from the separate machines; again no such effect was found.

The specimens used in this investigation were standard A.S.T.M. types, both notched and unnotched, and were prepared according to A.S.T.M. recommended procedures (ref. 10). The notched specimens had an outside diameter of 0.480 inch, an inside diameter of 0.300 inch, a notch angle of 60°, and a root radius of 0.020 inch. These specifications yield a specimen having a theoretical stress-concentration factor K_t of 2.25 (ref. 10). The unnotched specimens were standard R. R. Moore specimens having a $5\frac{1}{4}$-inch radius.

Preliminary tests on the notched material indicated that tests at five stresses per material would be appropriate. The stresses 12,500, 15,000, 20,000, 25,000, and 30,000 psi were used with only one exception; 13,500 psi was the minimum stress for the EL specimens because this class was so much stronger than the others at higher stresses that it was feared that at 12,500 psi many run-outs would be obtained; this would preclude the application of standard statistical techniques to these data. For the unnotched EL specimens tests were conducted at 40,000, 35,000, 30,000, and 25,000 psi. In three cases (RL, RT, and ET) where sufficient notched specimens remained following the main test work, statistical scatter checks were run at 20,000 psi. No tests were conducted for longer than 10^8 cycles and this number is used as the run-out point or point of truncation in the statistics. Ten specimens was the statistical sample size used in every test. The applicability of this sample size will be commented upon later in this report.

EXPERIMENTAL RESULTS AND DISCUSSION

The fatigue statistics for the four microstructures tested and also for the unnotched specimens are presented in tables II and III and the S-N curves are plotted in figures 7(a) to 7(d), with a summary plot of all notched data shown in figure 8. The original data are shown in table IV.

The statistical methods used were identical to those outlined by Epremian and Mehl (ref. 3). The only exception arose from the fact that aluminum alloys show no sharp endurance limit. At low stresses, using an arbitrary point of truncation, there would be some samples in which all the specimens did not break. In order to make use of all the specimens of a given sample, be they failures or run-outs, the censored logarithmic normal distribution was introduced. The method for the use of this type of statistic is briefly outlined in appendix A and further discussion of this method may be found in reference 11.

Ten specimens were tested at each stress and the logarithmic mean life $\overline{\log N}$, mean life $\overline{N}$, unbiased standard deviation σ, and the standard estimate of error $\sigma_{\overline{\log N}}$ determined for each group of specimens. The fatigue statistics for all specimen groups tested are given in table II. These statistics indicate a general increase in scatter with decreasing stress. At the higher stresses the extruded materials show less scatter than the recrystallized materials, but this trend disappears at 20,000 psi and below this stress level no meaningful trends are apparent.

The application of statistical tests of significance gives additional insight to the interpretation of the data of table II. The F test was

applied to the data to determine which form of the t test would be applicable.

The t test, at the 5-percent level of significance, which is used to test for a statistically significant difference between the mean values of two sets of measurements, was next applied to the data. A discussion of this test may be found in reference 11, page 397. The results of this test (table III) indicate that there exists a definite anisotropy in the fatigue strength of the extruded material at all stresses considered except the lowest, where an extrapolation was used. At the higher stresses there is no significant anisotropy in the fatigue strengths of the recrystallized material and only slight anisotropy at the lowest stress used. The three structures ET, RT, and RL are statistically identical at the higher stresses, but as the stress decreases it appears that the ET structure has a slightly higher fatigue strength.

Figures 7(a) to 7(c) show the S-N curves for the RT, ET, and RL specimens. Standing alone, these curves may be considered as typical of nonferrous fatigue behavior. Figure 7(d) shows the S-N curves for the EL specimens, both notched and unnotched. It can be seen that the theoretical stress-concentration factor is not solely responsible for the shift in S-N curves between the notched and unnotched specimens. The higher the stress, the closer is the behavior of the specimens to that which would be expected on the basis of the stress-concentration factor alone. Figure 7(d) shows that the fatigue-strength reduction factor K_f is equal to 2.22 at a life of 6×10^5 cycles and decreases with increasing logarithmic fatigue life until at 10^8 cycles its value is 1.54. This behavior obviously cannot persist to very short lifetimes; the limit was, however, not determined in this work.

It is noteworthy that Bruggeman, Mayer, and Smith (ref. 12) found the same general variation of the fatigue-strength reduction factor K_f with increasing stress in a comparable fatigue-life range (2×10^4 to 10^7 cycles) in 24S-T4 sheet tested in axial tension-compression.

Figure 8 is a summary graph of all the notched specimens. This graph clearly shows the anisotropy in the mean fatigue life existing in the extruded structure. It should be noted that one fatigue curve fits the data of the three remaining structures almost as well as would three separate curves. This representation is satisfactory at the higher stresses on the basis of the results of the t test and breaks down completely only at the lowest stress (12,500 psi). It is also interesting to note the apparent sensitivity of notched fatigue tests to differences in tensile strength. In the range of finite life there is an appreciable difference of fatigue life accompanying a similar difference in tensile strength (as between EL and ET). Cazaud (ref. 13, p. 188) shows

this when referring to the work of Pomey and Ancelle on a quenched and tempered nickle-chromium steel. Where the difference in tensile strengths is small between structures (RT, ET, and RL), the difference in fatigue lives is also small. S-N diagrams for longitudinal and transverse notched specimens of this same steel show behavior identical to that of the EL and ET specimens, even to the meeting of the curves at long fatigue lives and the anisotropy in fatigue life at high stresses. The observed displacement of the three lower strength materials (ET, RL, and RT) at the lower stresses is of unknown significance; the present authors are not fully convinced of its validity. The authors do not know whether the observed displacement of the EL structure from the other three structures should persist to long lifetimes (low stresses) or not. The data are equivocal; the displacement is observed and on a consistency basis might be assumed, but the scatter at low stresses is so large as to give no statistically significant results.

A survey of the fractures obtained in the testing of the four types of specimens yields some interesting observations. The transverse specimens (both ET and RT) exhibit a common type of fracture at the higher stresses. The area of final fracture for these specimens was elliptical in shape and one end of the major axis of the ellipse was in the position on the fracture cross section where the fibers were the shortest (figs. 9(a) and 9(b). The characteristic features of the fatigue crack were that it appeared to have begun at the root of the notch and spread completely around the notch perimeter. Another feature of the area of final fracture was that a line drawn through the major axis of the fracture ellipse was perpendicular to the fiber direction. These observations suggest that the rate of propagation of the fatigue crack is anisotropic, being faster in the fiber direction. They suggest further that the initial fatigue crack was often generated at the point where the fiber length was the shortest. This might well be expected since this is the position where a proper notch would be most difficult to make.

Most of the exceptions to the above observations occurred at the lower stresses where the position of the final failure was almost random (fig. 9(b)). However, in many cases at the lower stresses the final failure was near the position of longest fibers (fig. 9(a)). When this was the case, the major axis of the elliptical area of final failure was still perpendicular to the fiber direction (fig. 9(a)). In all cases it appeared as if the effective stress concentration was more pronounced at the higher stresses - the higher the stress, the smaller was the area of the fatigue crack. This observation is in agreement with that previously mentioned for the decrease of the fatigue-strength reduction factor with increasing fatigue life (and decreasing stress) found for the notched and unnotched EL specimens. The appearance of the fibers was more ragged in the fractures of the recrystallized specimens, indicating a relief of elastic stresses in this material and thus more of a tendency for the cracked fibers to smear. Another indication of the relief of stress due

to recrystallization was that the perpendicular rule appeared to have fewer exceptions in these fractures; thus the fracture position was less influenced by small differences in the structures.

Figures 10(a) and 10(b) show fractures typical of the longitudinal specimens (EL and RL). As the test stress increased, the area of final failure became more centrally located in the cross section of the notch and also tended to be more circular. Here, also, the smooth area increased with increasing stress, and the effect of stress concentration was more pronounced at the higher stresses. In these fractures the cracked area appeared to proceed radially, as would be expected from the random nature of the microstructure and the radial nature of the stress gradient. The two extra fractures in figure 10(a) are exceptions, presumably indicating that some other factor can upset these general rules.

Figures 11(a) and 11(b) show the various fracture types obtained with the unnotched specimens. The fractures shown in figure 11(a) are "ideal" fatigue fractures and are typical of those found in unnotched specimens. The "odd" fractures shown in figure 11(b) can be explained on the basis of the fibrous nature of the material which would favor angular propagation instead of propagation perpendicular to the specimen axis, coupled, perhaps, with residual surface stresses (ref. 14).

The fact that the notched specimens exhibited considerably less scatter than the unnotched (at the same stress) sheds some further light on the failure theory of Epremian and Mehl (ref. 2). In view of this theory two stands can be taken with respect to the effect of a notch in fatigue specimens. First, it would seem that the scatter in probability of failure would be greater for a specimen where the location of failure is constrained by a notch. Second, and conversely, the stress concentration and high stress gradient produced by the notch would correspond to the high-stress condition of the theory and hence would lead to a smaller scatter. In fact, it seems as if the second condition overshadows the first in this particular alloy under the given testing conditions. The assumption is implicit, however, in the definition of a "fatigue-strength reduction factor" that equal stresses cause an equal effect in the same material, that is, that the notch "apparently" concentrates the applied stress until it is the equal of the applied stress in an unnotched specimen that has the same life. This is probably a good assumption as applied to crack initiation and, therefore, to fatigue limits, rather than to fatigue lives which also include crack propagation. Applied at face value, however, the assumption militates against ascribing the lower observed scatter in notched specimens to a "higher" stress; at the same life (cycles to failure N) the actual stress involved is the same in notched and unnotched specimens.

It implies, too, that the comparison of scatter ought to be made at constant cycles to failure rather than at constant applied stress.

Tested in this way the present data appear to show, but not unequivocally, that the unnotched specimens still exhibit larger statistical scatter than the notched specimens, at least at the shorter lives.

However, once a fatigue crack has been formed in both the notched and unnotched specimens, the stress concentration will be the same and the actual stress operating to propagate the crack will be less in the unnotched specimen because of the lower applied load. On the basis of much recent work showing that crack propagation accounts for much the larger fraction of cycles to failure, this would be expected to be the larger effect.

One recourse is available. It can be assumed that the steeper stress gradient and/or the different state of stress in the notched specimen (rather than the magnitude of the maximum stress) are responsible. The secondary tensile stresses brought about by the notch can be expected to make available more sites for the creation of a fatigue crack. The observed decrease in scatter in cycles to failure is then traceable to a decrease in the scatter of cycles to initiate a fatigue crack rather than in those cycles to propagate it.

Generally, the statistical scatter appears to increase with decreasing stress. The fact that this did not hold true in all cases is believed to be due to the fact that an insufficient number of specimens were tested at any given stress level. This is further evidenced by the fact that scatter checks showed widely (statistically significant) different means and standard deviations in some cases and not in others (table II). The authors believe that a minimum of 20 specimens at a stress is necessary to give reproducible statistics. This suggestion has been made several times in the past.

That the scatter checks showed statistically significant different means and standard deviations could be accepted as evidence that the two samples (10 specimens each) were drawn from different populations, that is, that the material changed with time or that the testing procedure changed. The authors are convinced that neither of these is tenable. Obviously there is always a finite chance in any sampling procedure of getting a "biased" sample. It is felt that this is what has occurred. The authors' experience would indicate that with a larger sample (20 specimens) the probability of this happening is lowered even beyond the amount guaranteed by statistical theory.

CONCLUSIONS

A study was made of the effects of microstructure and anisotropy on the fatigue of notched specimens of 24S-T4 aluminum alloy. Within the limitations of the test conditions and on the basis of the information obtained, the following conclusions are drawn:

1. A definite anisotropy in the notched fatigue strength exists in extruded 24S-T4 specimens; this anisotropy decreases with decreasing stress level.

2. No significant anisotropy exists in the fatigue strength of 24S-T4 notched specimens extruded and recrystallized at higher stress levels; some anisotropy may appear at the lower stress levels.

3. The fatigue strength of the extruded and recrystallized 24S-T4 notched specimens is essentially the same as that of the extruded material in the transverse direction.

4. The fatigue-strength reduction factor K_f for a notch with a theoretical stress-concentration factor K_t of 2.25 decreases with decreasing stress in the extruded material tested with longitudinal specimens.

5. There is more statistical scatter in cycles to failure in unnotched specimens than in the notched specimens. This effect must be ascribed to higher stress gradient or to the triaxiality of the state of stress introduced by the notch.

6. At higher stresses the extruded materials possess smaller statistical scatter than do the recrystallized materials, but this trend disappears at and below 20,000 psi and no further significant trends can be found.

7. Generally, the statistical scatter appears to increase with decreasing stress level.

8. For the transverse specimens the area of final fracture was elliptical in shape; a line drawn through the major axis of the ellipse was perpendicular to the fiber axis, and one end of the major axis of the crack ellipse was just under the surface of the notch.

9. For the longitudinal specimens the area of final fracture was more circular than elliptical, and this area was generally more centrally located on the cross section.

10. A sample size of 10 specimens does not give statistically reproducible results in all cases. It is believed that a minimum sample size of 20 specimens should be used in all further investigations of this type on aircraft construction materials.

Carnegie Institute of Technology,
Pittsburgh, Pa., September 30, 1953.

APPENDIX A

CENSORED LOGARITHMIC NORMAL DISTRIBUTION[1]

The censored logarithmic normal type of distribution is a special case of the logarithmic normal distribution (used for all previous fatigue statistics) with which the entire population may still be sampled, but individual values of observation below or above a given value are not specified. The specific application of this distribution to fatigue testing is in tests of nonferrous alloys at low stress levels where the fatigue testing may extend beyond 10^8 cycles and the dispersion in fatigue life may be rather large. Out of 10 specimens tested at this low stress level 8 might fail before 10^8 cycles, a test duration set by practical considerations only. However, experience indicates that the remaining two specimens would eventually fail after some additional cycles. Calculation of $\overline{\log N}$ and σ on the basis of only those specimens which failed would not provide a true picture of the situation. The consideration of a censored distribution allows the calculation of the required statistics making use of all the available data.

A word of caution should be given lest this method be assumed applicable to the problem encountered with steel where a small number of run-outs occur at the lowest stress in the fracture range when the finite-life statistics overlap with the statistical range of the endurance limit. For the case of a true endurance limit the gap in cycles between the life of specimens which fail and the life of run-outs, 2.5 or 5×10^7 cycles, is so great that the run-outs cannot be considered as belonging to the same population as that of the specimens which failed.

Hald (ref. 11) discusses the censored normal distribution on page 149. His analysis can be used with the logarithmic normal distribution simply by making the transformation $x = \log N$. The following equations will be given in terms of $\log N$.

Consider n specimens tested at the stress to be divided into two groups: a specimens which had not failed at the point of truncation and $n - a$ specimens which failed. The degree of truncation h is given by equation (1):

---

[1]The material for this entire section was taken from the Doctorate Thesis of G. E. Dieter entitled "Further Investigations Upon the Statistical Nature of the Fatigue of Metals," Carnegie Institute of Technology, May 28, 1953 (ref. 16). The material, as here presented, was adapted slightly to the present needs.

$$h = a/n \tag{1}$$

Next, calculate the parameter y from equation (2):

$$y = \frac{(n - a)\sum_{1}^{n-a} x_i^2}{2\left(\sum_{1}^{n-a} x_i\right)^2} \tag{2}$$

where

x_i $\log N_c - \log N_i$

N_c point of truncation

Having calculated y, an estimate of the standardized point of truncation z, which is a function of h and y, is obtained from table X in reference 15. An estimate of the standard deviation is calculated from equation (3):

$$\sigma = \frac{\sum_{1}^{n-a} x_i}{n - a}\, g(h,z) \tag{3}$$

where the function $g(h,z)$ is obtained from table X, reference 15. The mean of $\log N$ at this stress is then calculated from equation (4):

$$\overline{\log N} = \log N_c + z\sigma \tag{4}$$

From this point on the remaining statistics are found in the usual way. The use of this method gives slightly greater mean values and standard deviations than would be obtained by using only the fractured specimens. The increased value of the standard deviation is in better agreement with what other investigators have reported for the scatter in fatigue life for aluminum alloys at low stresses.

REFERENCES

1. Ransom, J. T., and Mehl, R. F.: The Statistical Nature of the Endurance Limit. Jour. Metals, vol. 1, no. 6, June 1949, pp. 364-365.

2. Epremian E., and Mehl, R. F.: Investigation of Statistical Nature of Fatigue Properties. NACA TN 2719, 1952.

3. Dieter, G. E., and Mehl, R. F.: Investigation of the Statistical Nature of the Fatigue of Metals. NACA TN 3019, 1953.

4. Dieter, G. E., Horne, G. T., and Mehl, R. F.: Statistical Study of Overstressing in Steel. NACA TN 3211, 1954.

5. Ravilly, E.: Contribution à l'etude de la rupture des fils métalliques soumis à des torsions alternées. Pub. sci. et tech., Ministère de l'air, no. 120, 1938, pp. 52-70.

6. Yen, C. S., and Dolan, T. J.: An Experimental Study of the Effect of Thermal Activation on the Fatigue of 75S-T Aluminum Alloy. Twelfth Prog. Rep. on An Investigation of the Behavior of Materials Under Repeated Stress, Contract N6-ori-71, Task Order IV, Office of Naval Res. and Eng. Exp. Station, Univ. of Ill., Oct. 1949.

7. Dolan, T. J., and Brown, H. F.: Effect of Prior Repeated Stressing on the Fatigue Life of 75S-T Aluminum. Preprint 91, A.S.T.M., 1952.

8. Head, A. K.: Statistical Properties of Fatigue Data on 24S-T Aluminum Alloy. Bull. No. 169, A.S.T.M., 1950, pp. 51-53.

9. Templin, R. L., Howell, F. M., and Hartmann, E. C.: Effect of Grain Direction on Fatigue Properties of Aluminum Alloys. Product Eng., vol. 21, no. 7, July 1950, pp. 126-130.

10. Committee E-9 on Fatigue: Manual on Fatigue Testing. Special Tech. Pub. No. 91, A.S.T.M., Dec. 1949, p. 33.

11. Hald, A.: Statistical Theory With Engineering Applications. John Wiley & Sons, Inc., 1952.

12. Brueggeman, W. C., Mayer, M., Jr., and Smith, W. H.: Axial Fatigue Tests at Zero Mean Stress of 24S-T Aluminum Alloy Sheet With and Without a Circular Hole. NACA TN 955, 1944.

13. Cazaud, R., (A. J. Fenner, trans.): Fatigue of Metals. Chapman & Hall, Ltd. (London), 1953.

14. Hetényi, M., ed.: Handbook of Experimental Stress Analysis. John Wiley & Sons, Inc., 1950, p. 529.

15. Hald, A.: Statistical Tables and Formulas. John Wiley & Sons, Inc., 1952, p. 64.

16. Dieter, G. E.: Further Investigations Upon the Statistical Nature of the Fatigue of Metals. Doctorate Thesis, Carnegie Inst. Tech., May 28, 1953.

TABLE I

MECHANICAL PROPERTIES[a] OF 24S-T4 ALUMINUM ALLOY

Material	Ultimate tensile strength, psi	Yield strength (0.2-percent offset), psi	Elongation, percent	Brinell hardness (10-mm ball, 500-kg load, 30 sec)[b]
Extruded-longitudinal	80,650	61,250	14.6	100
Recrystallized-longitudinal	67,950	52,600	19.8	93
Extruded-transverse	71,700	52,750	14.2	96
Recrystallized-transverse	67,950	46,100	11.9	89

[a]Average of five tests.

[b]Measurements made on surfaces shown in figures 5(b), 5(d), 6(a), and 6(b).

TABLE II

FATIGUE STATISTICS FOR 24S-T4 ALUMINUM ALLOY

Specimen	Stress, psi	Mean life, $\overline{N}$	Unbiased standard deviation, σ	Standard estimate of error, $\sigma_{\overline{\log N}}$
Notched specimens				
EL	30,000	4.28×10^5	0.04347	0.01375
RL		6.18×10^4	.13475	.04262
ET		7.64	.09231	.02919
RT		6.96	.13382	.04232
EL	25,000	5.09×10^5	.05375	.01699
RL		1.11	.07927	.02507
ET		1.17	.06556	.02073
RT		1.30	.13495	.04268
EL	20,000	8.32	.05173	.01636
RL		3.02	.07409	.02343
ET		3.07	.08067	.02551
RT		2.22	.06874	.02174
EL	15,000	1.75×10^6	.13792	.04362
RL		4.66	.16758	.05299
ET		4.91	.43192	.13659
RT		3.12	.47303	.14959
EL	13,500	2.94×10^7	.31375	.09922
RL	12,500	1.69	.16977	.05368
ET	12,500	7.85	.20945	.06623
RT	12,500	2.72	.24569	.07769
[a]RL	20,000	1.53×10^5	.11503	.03638
[a]ET		2.76	.03011	.00952
[a]RT		1.52	.11121	.03517
[b]RL		2.15	.17832	.03987
[b]ET		2.91	.06375	.01425
[b]RT		1.84	.12399	.02773
Unnotched specimens				
EL	40,000	1.50×10^6	0.14176	0.04483
	35,000	2.61	.26571	.08403
	30,000	4.91	.16234	.05133
	25,000	1.36×10^7	.17051	.05392

[a]Scatter check; 10 specimens.

[b]Scatter check; total of 20 specimens.

TABLE III

RESULTS OF t TEST

Materials compared	Stress, psi				
	30,000	25,000	20,000	15,000	12,500
$\frac{RT}{ET}$	N.S.D.	N.S.D.	S.D.	N.S.D.	S.D.
$\frac{RT}{RL}$	N.S.D.	N.S.D.	S.D.	N.S.D.	S.D.
$\frac{ET}{RL}$	Slight S.D.	N.S.D.	N.S.D.	N.S.D.	S.D.
Strongest material at stress / EL	$\frac{ET}{EL}$, S.D.	$\frac{RT}{EL}$, S.D.	$\frac{ET}{EL}$, S.D.	$\frac{ET}{EL}$, S.D.	[a] $\frac{ET}{EL}$, N.S.D.

[a] EL curve extrapolation to 12,500 psi yields 7×10^7; calculation made on this basis.

TABLE IV

RESULTS OF ROTATING-BEAM FATIGUE TESTS OF 24S-T4 ALUMINUM ALLOY

(a) Notched extruded longitudinal specimens

Specimen	Cycles to failure, N	Specimen	Cycles to failure, N	Specimen	Cycles to failure, N
30,000 psi		25,000 psi		20,000 psi	
EL-33	5.34×10^5	EL-27	4.45×10^5	EL-45	8.21×10^5
EL-14	4.08	EL-79	5.21	EL-9	9.87
EL-60	4.41	EL-26	4.77	EL-51	7.92
EL-18	4.00	EL-80	5.08	EL-32	7.39
EL-29	3.81	EL-61	4.50	EL-57	8.78
EL-19	4.58	EL-81	5.13	EL-59	7.58
EL-71	4.29	EL-43	5.68	EL-6	8.29
EL-5	4.28	EL-82	5.58	EL-53	1.031×10^6
EL-72	3.80	EL-28	4.38	EL-55	7.12×10^5
EL-8	4.43	EL-83	6.46	EL-46	8.27

Specimen	Cycles to failure, N	Specimen	Cycles to failure, N
15,000 psi		13,500 psi	
EL-63	1.1994×10^7	EL-52	1.8610×10^7
EL-25	1.6949	EL-41	2.6702
EL-10	2.8493	EL-12	5.5165
EL-48	1.2366	EL-38	Run-out
EL-7	2.0990	EL-74	1.7717
EL-56	1.8253	EL-4	1.6408
EL-76	1.8646	EL-36	4.1731
EL-49	2.0320	EL-39	2.1681
EL-73	1.0856	EL-27	4.3529
EL-58	2.4628	EL-64	1.1894

TABLE IV.- Continued

RESULTS OF ROTATING-BEAM FATIGUE TESTS OF 24S-T4 ALUMINUM ALLOY

(b) Notched recrystallized longitudinal specimens

Specimen	Cycles to failure, N	Specimen	Cycles to failure, N	Specimen	Cycles to failure, N
30,000 psi		25,000 psi		20,000 psi	
RL-38	4.4×10^4	RL-54	9.3×10^4	RL-75	3.10×10^5
RL-14	5.4	RL-60	8.5	RL-46	3.62
RL-18	8.5	RL-71	1.19×10^5	RL-42	3.55
RL-11	5.3	RL-12	9.8×10^4	RL-58	2.11
RL-53	7.9	RL-73	1.06×10^5	RL-25	2.85
RL-23	5.1	RL-4	1.61	RL-8	3.39
RL-57	8.2	RL-26	1.25	RL-59	2.50
RL-49	3.7	RL-74	1.27	RL-45	3.14
RL-15	9.2	RL-13	1.10	RL-44	2.91
RL-56	6.8	RL-51	1.04	RL-7	3.46
Specimen	Cycles to failure, N	Specimen	Cycles to failure, N	Specimen	Cycles to failure, N
15,000 psi		12,500 psi		[a]20,000 psi	
RL-61	5.756×10^6	RL-37	2.5702×10^7	RL-19	1.35×10^5
RL-5	4.075	RL-33	1.7468	RL-3	1.36
RL-41	2.092	RL-72	1.2467	RL-48	1.07
RL-28	2.924	RL-22	2.6890	RL-10	2.26
RL-17	5.071	RL-63	2.1763	RL-66	1.22
RL-40	6.001	RL-16	1.4878	RL-69	1.64
RL-34	6.360	RL-65	8.644×10^6	RL-76	1.26
RL-6	7.434	RL-9	1.7398×10^7	RL-36	2.36
RL-47	5.472	RL-39	2.4972	RL-29	1.86
RL-64	4.279	RL-67	1.0716	RL-43	1.46

[a]Scatter check.

TABLE IV.- Continued

RESULTS OF ROTATING-BEAM FATIGUE TESTS OF 24S-T4 ALUMINUM ALLOY

(c) Notched extruded transverse specimens

Specimen	Cycles to failure, N	Specimen	Cycles to failure, N	Specimen	Cycles to failure, N
30,000 psi		25,000 psi		20,000 psi	
ET-21	5.5×10^4	ET-54	1.16×10^5	ET-72	2.70×10^5
ET-46	1.19×10^5	ET-10	1.28	ET-41	2.72
ET-62	7.6×10^4	ET-78	1.14	ET-27	2.18
ET-32	7.8	ET-22	1.13	ET-19	3.94
ET-65	9.1	ET-17	1.32	ET-24	3.57
ET-66	6.3	ET-77	1.17	ET-73	2.58
ET-58	8.3	ET-30	9.5×10^4	ET-26	3.22
ET-11	7.6	ET-76	1.61×10^5	ET-60	3.71
ET-13	7.4	ET-57	1.04	ET-56	3.18
ET-52	6.5	ET-3	1.01	ET-34	3.35
Specimen	Cycles to failure, N	Specimen	Cycles to failure, N	Specimen	Cycles to failure, N
15,000 psi		12,500 psi		[a]20,000 psi	
ET-14	1.3069×10^7	ET-48	Run-out	ET-43	2.30×10^5
ET-40	1.298×10^6	ET-29	8.3507×10^7	ET-79	2.78
ET-42	3.840	ET-68	Run-out	ET-47	2.78
ET-6	1.8969×10^7	ET-37	Run-out	ET-80	2.87
ET-31	8.79×10^5	ET-53	8.4208×10^7	ET-28	2.91
ET-61	4.941×10^6	ET-4	8.6230	ET-81	2.93
ET-18	7.942	ET-2	4.1057	ET-8	2.74
ET-9	2.626	ET-74	5.6413	ET-63	2.88
ET-7	1.0618×10^7	ET-64	3.8276	ET-82	2.73
ET-67	6.850×10^6	ET-16	6.9365	ET-83	2.75

[a]Scatter check.

TABLE IV.- Continued

RESULTS OF ROTATING-BEAM FATIGUE TESTS OF 24S-T4 ALUMINUM ALLOY

(d) Notched recrystallized transverse specimens

Specimen	Cycles to failure, N	Specimen	Cycles to failure, N	Specimen	Cycles to failure, N
30,000 psi		25,000 psi		20,000 psi	
RT-58	1.00×10^5	RT-30	8.2×10^4	RT-49	2.11×10^5
RT-8	6.2×10^4	RT-2	1.65×10^5	RT-19	2.05
RT-59	1.10×10^5	RT-12	1.24	RT-17	2.14
RT-45	4.1×10^4	RT-22	1.52	RT-57	2.11
RT-51	7.3	RT-26	1.20	RT-54	2.15
RT-31	9.6	RT-33	9.2×10^4	RT-18	2.46
RT-44	6.4	RT-40	1.93×10^5	RT-11	1.72
RT-7	5.8	RT-66	1.74	RT-14	2.10
RT-63	6.9	RT-10	8.9×10^4	RT-56	2.53
RT-41	5.3	RT-74	1.67×10^5	RT-65	3.12
Specimen	Cycles to failure, N	Specimen	Cycles to failure, N	Specimen	Cycles to failure, N
15,000 psi		12,500 psi		[a]20,000 psi	
RT-34	7.12×10^5	RT-4	6.0462×10^7	RT-25	1.53×10^5
RT-6	6.465×10^6	RT-64	3.1606	RT-73	1.10
RT-62	1.3363×10^7	RT-21	1.4855	RT-69	2.12
RT-24	1.066×10^6	RT-39	1.5772	RT-52	1.32
RT-47	3.040	RT-5	5.8089	RT-27	1.12
RT-75	1.0344×10^7	RT-13	4.7712	RT-60	2.18
RT-72	1.849×10^6	RT-37	2.4603	RT-15	1.22
RT-46	4.451	RT-28	3.0417	RT-9	1.42
RT-42	7.23×10^5	RT-23	1.4367	RT-48	1.61
RT-68	7.289×10^6	RT-61	1.6740	RT-3	2.00

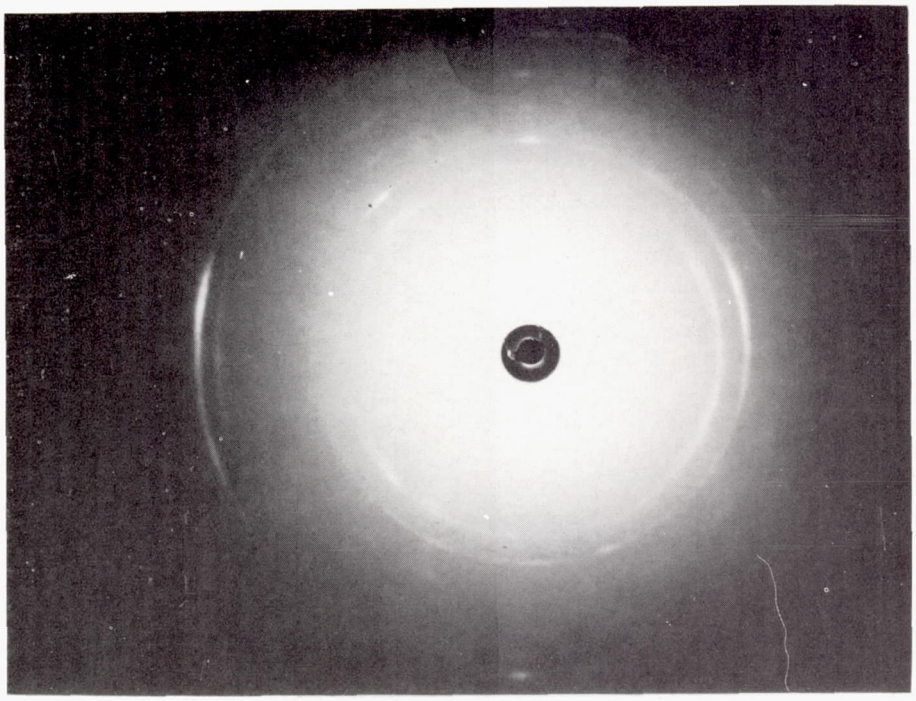
[a]Scatter check

TABLE IV.- Concluded

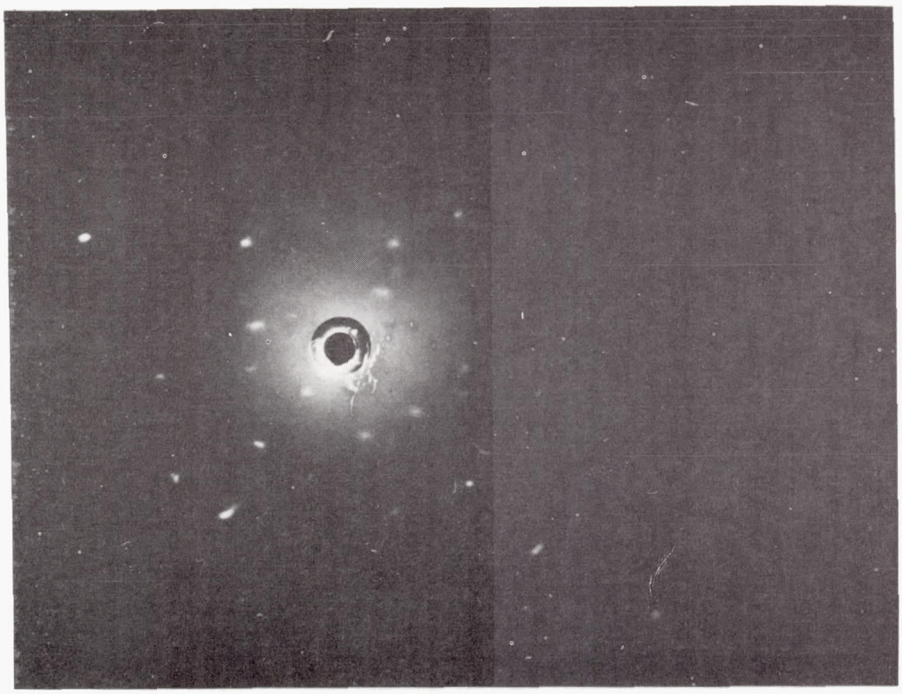
RESULTS OF ROTATING-BEAM FATIGUE TESTS OF 24S-T4 ALUMINUM ALLOY

(e) Unnotched extruded longitudinal specimens

Specimen	Cycles to failure, N	Specimen	Cycles to failure, N
40,000 psi		35,000 psi	
EL-100-U	9.90×10^5	EL-77-U	3.154×10^6
EL-92-U	1.208×10^6	EL-82-U	1.308
EL-115-U	2.201	EL-89-U	5.402
EL-90-U	1.424	EL-112-U	1.576
EL-98-U	1.342	EL-106-U	1.836
EL-95-U	1.300	EL-108-U	1.983
EL-109-U	2.754	EL-93-U	4.416
EL-104-U	1.272	EL-83-U	1.177
EL-111-U	1.271	EL-79-U	6.788
EL-81-U	1.991	EL-105-U	3.254
Specimen	Cycles to failure, N	Specimen	Cycles to failure, N
30,000 psi		25,000 psi	
EL-87-U	4.806×10^6	EL-101-U	9.995×10^6
EL-94-U	3.629	EL-85-U	3.1191×10^7
EL-84-U	3.176	EL-113-U	9.164×10^6
EL-99-U	4.335	EL-103-U	1.1047×10^7
EL-96-U	4.980	EL-86-U	1.4636
EL-88-U	7.477	EL-107-U	1.8591
EL-78-U	9.574	EL-110-U	1.1199
EL-91-U	6.810	EL-80-U	1.5798
EL-102-U	4.585	EL-97-U	1.6294
EL-116-U	3.053	EL-114-U	8.616×10^6



(a) Extruded.

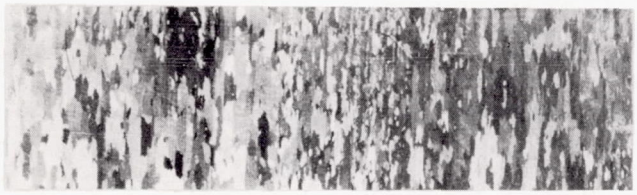


(b) Recrystallized.

Figure 1.- Laue back-reflection photograms of 24S-T4 aluminum alloy.

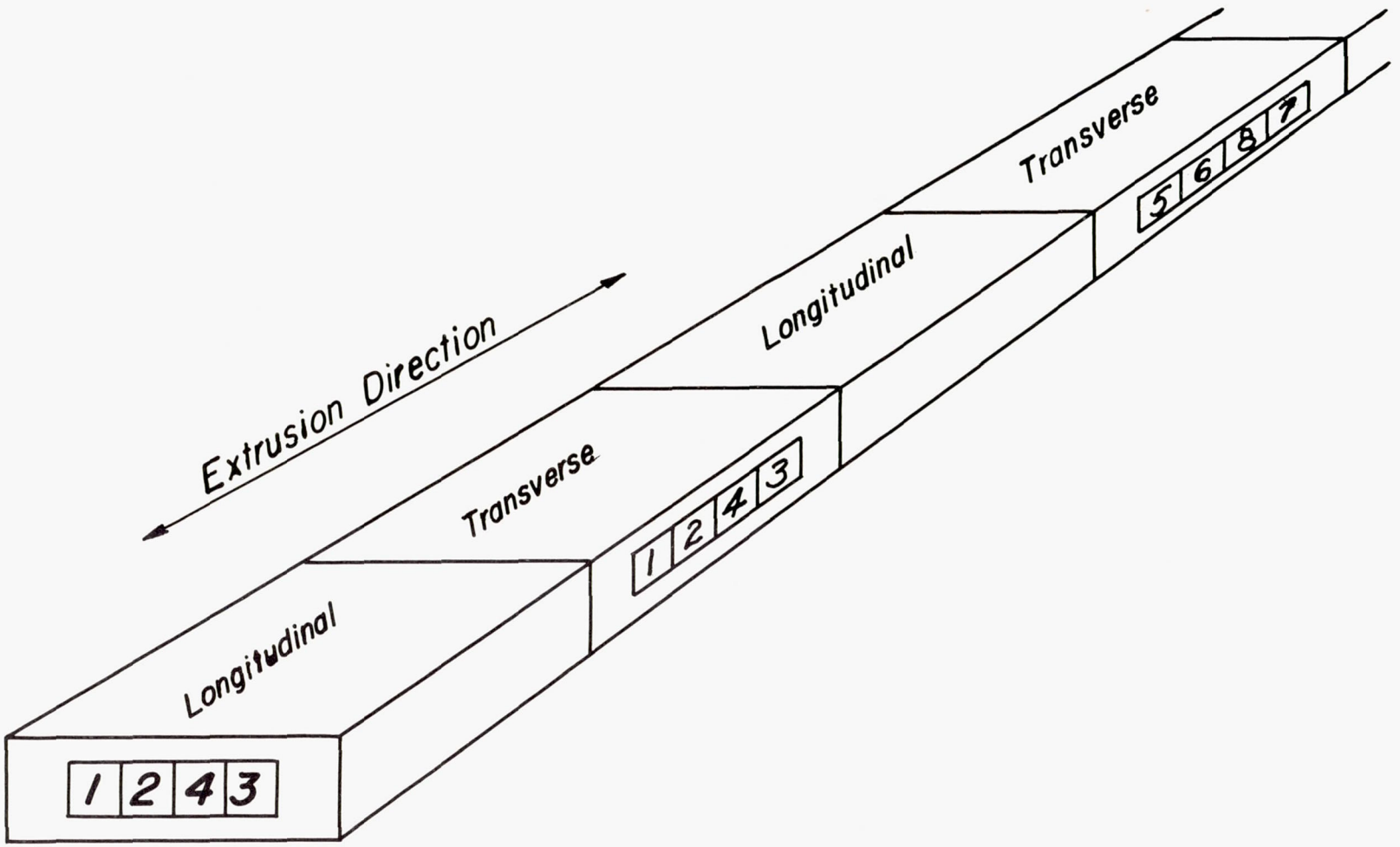


(a) End view.



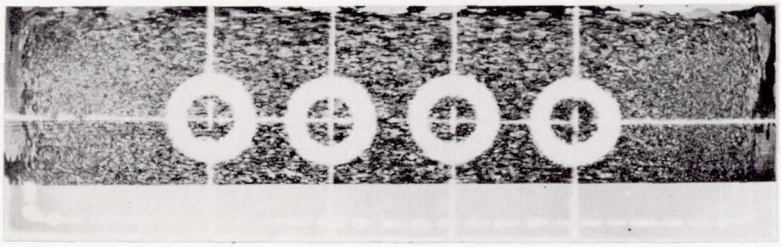
(b) Top view.

Figure 2.- Views of extruded 24S-T4 aluminum-alloy bar stock. Etched in modified Keller's etch; 1X.

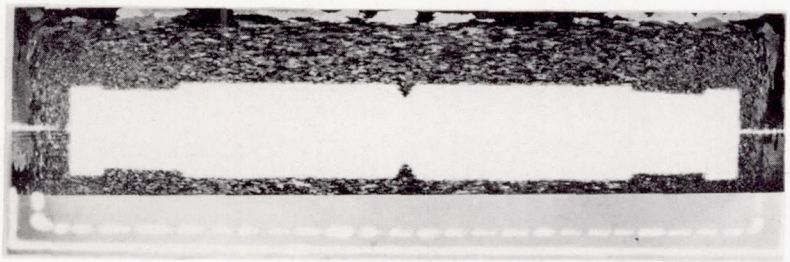


(a) Bar layout for specimens.

Figure 3.- Position of specimens in original 24S-T4 aluminum-alloy bar stock.

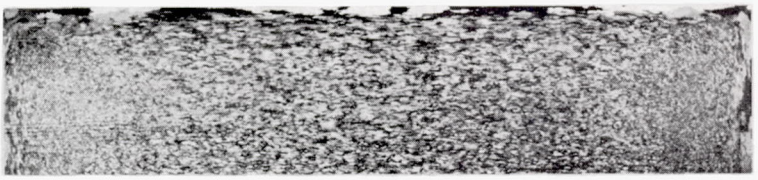


(b) Position of longitudinal specimens.



(c) Position of transverse specimens.

Figure 3.- Concluded.

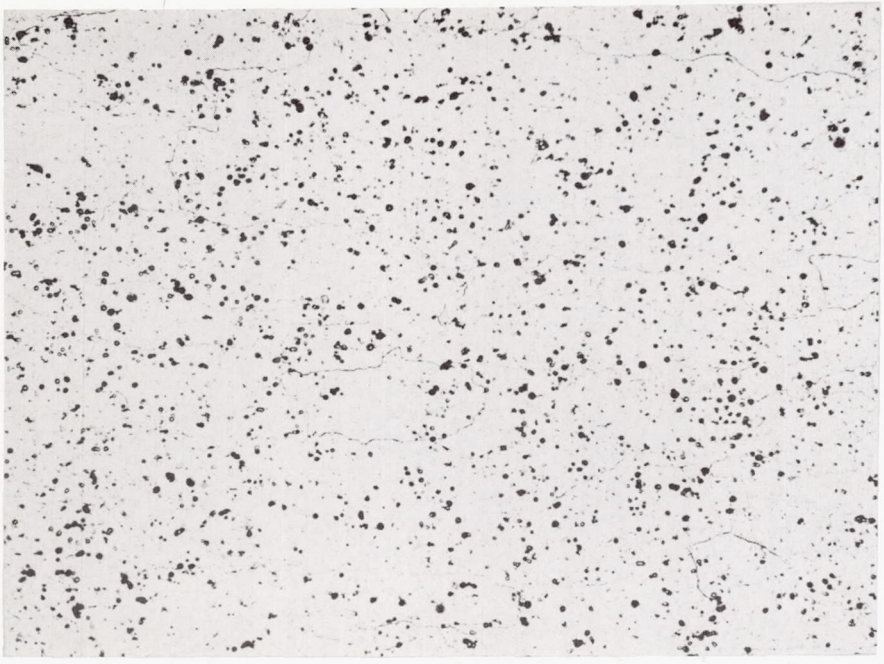


(a) End view.

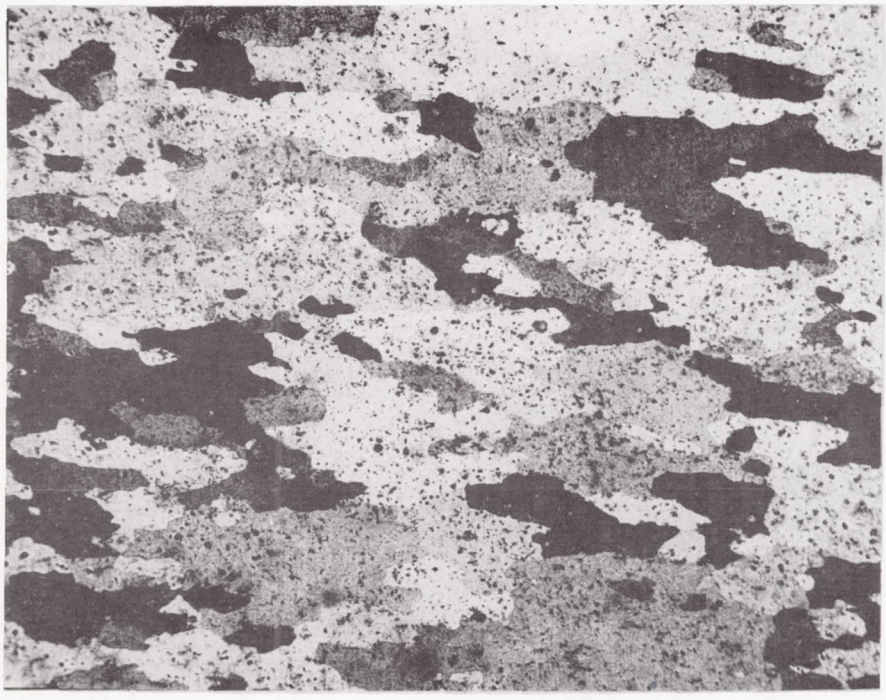


(b) Top view.

Figure 4.- Views of recrystallized 24S-T4 aluminum-alloy bar stock. Etched in modified Keller's etch; 1X.

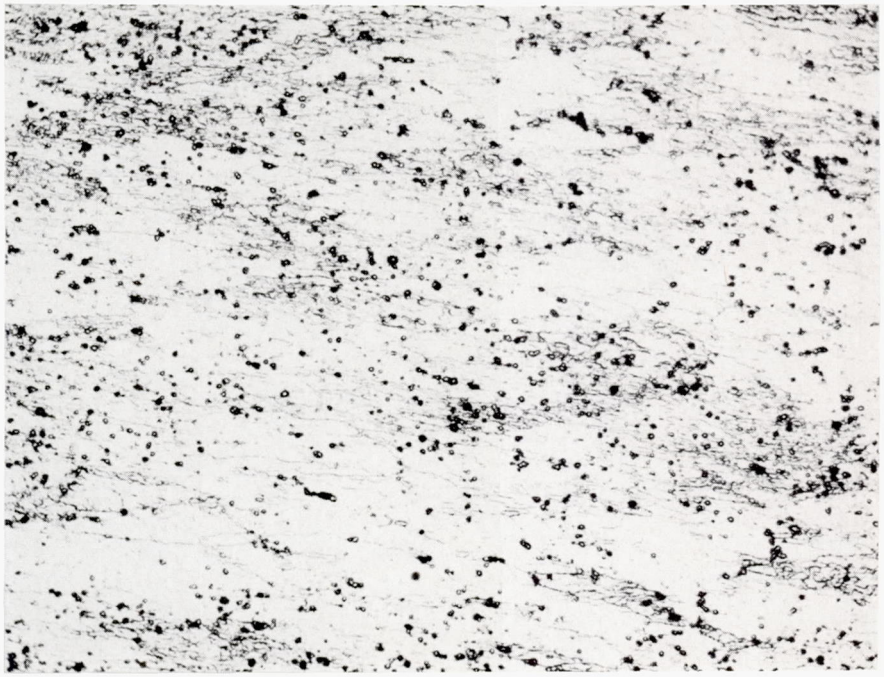


(a) Recrystallized transverse specimens. Unetched; 100X.

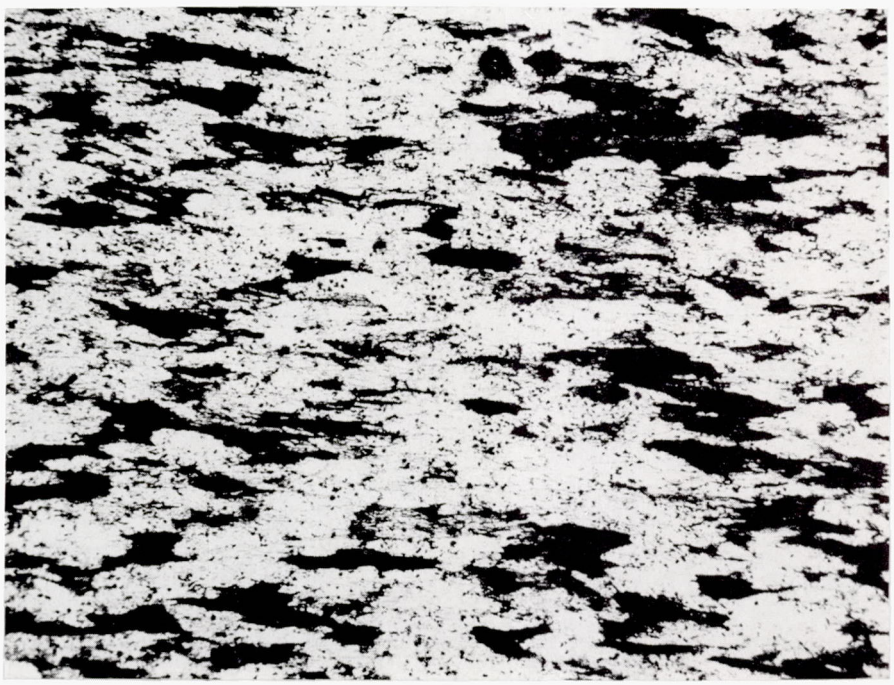


(b) Recrystallized transverse specimens. Etched in Keller's etch; 50X.

Figure 5.- Typical microstructures, unetched and etched, of longitudinal and transverse specimens of 24S-T4 aluminum alloy.



(c) Extruded transverse specimens. Unetched; 100X.



(d) Extruded transverse specimens. Etched in Keller's etch; 50X.

Figure 5.- Continued.

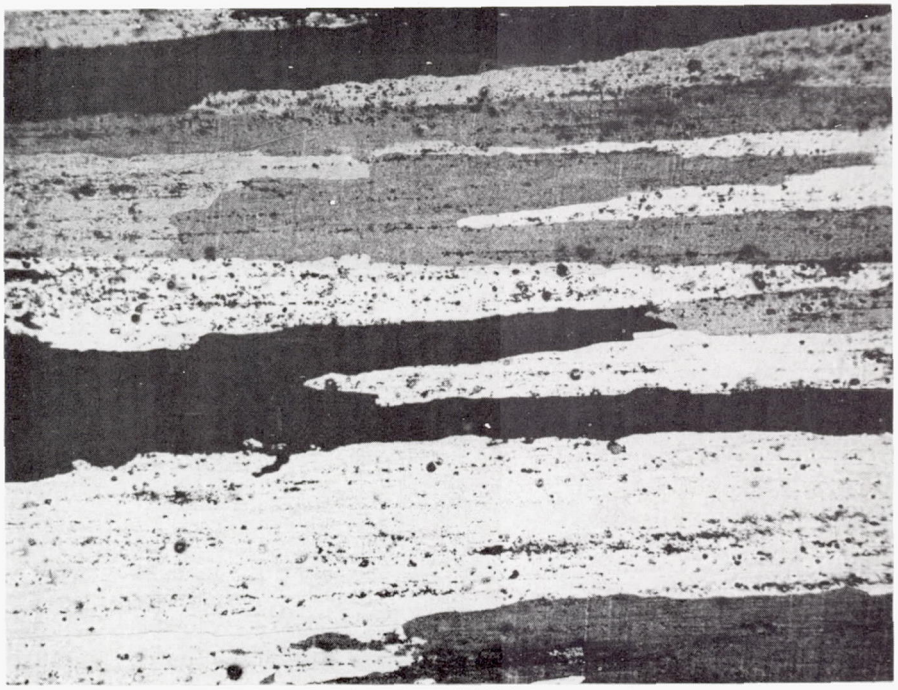


(e) Extruded longitudinal specimens. Unetched; 100X.



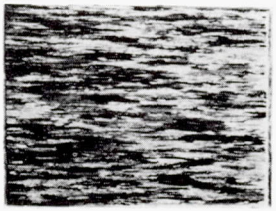
(f) Recrystallized longitudinal specimens. Unetched; 100X.

Figure 5.- Continued.

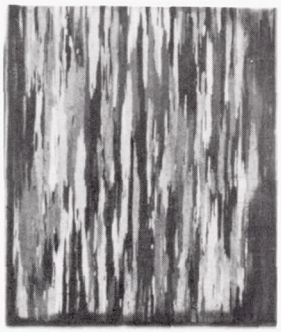


(g) Recrystallized longitudinal specimens. Etched in Keller's etch; 50X.

Figure 5.- Concluded.

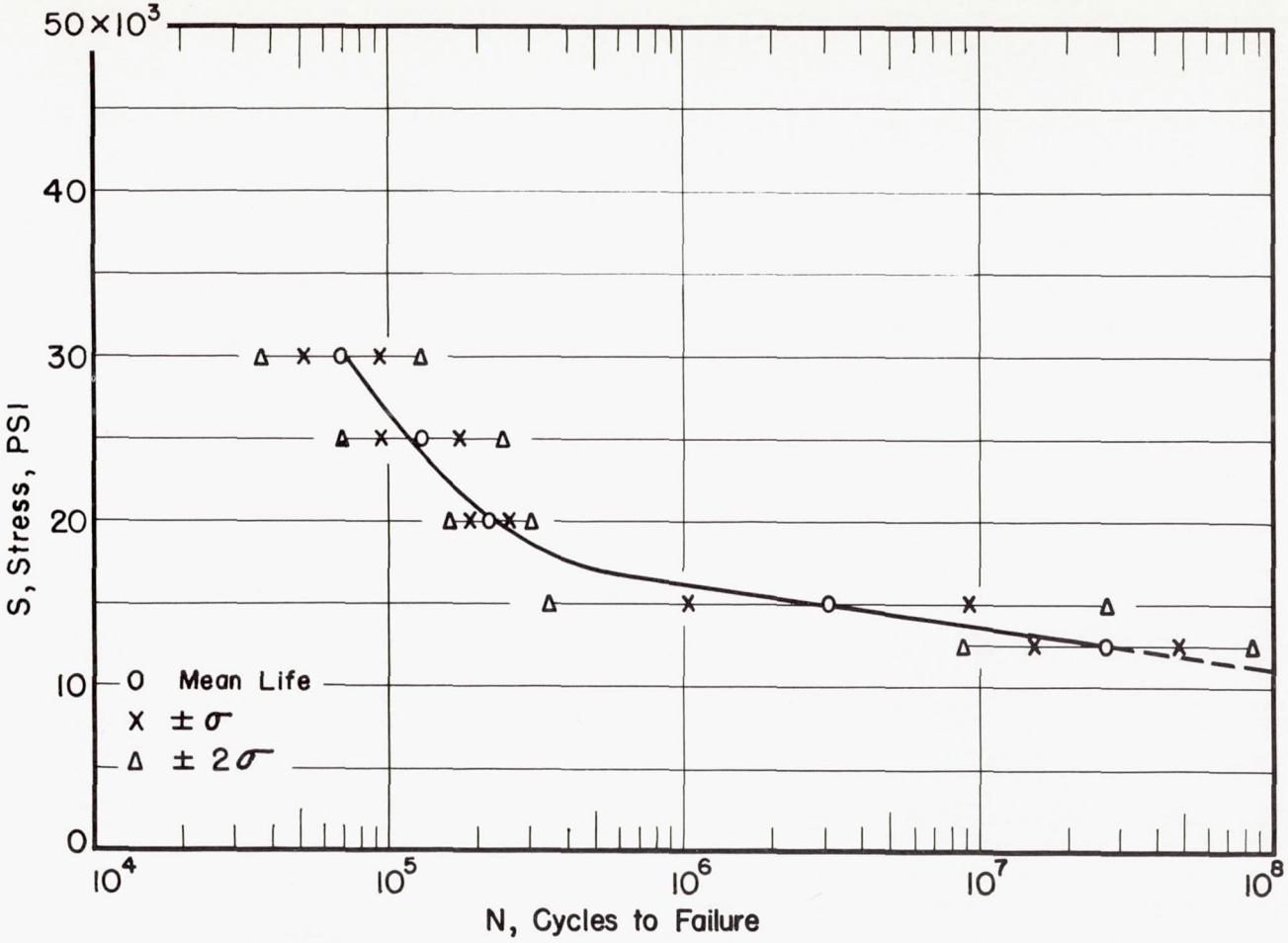


(a) Extruded.



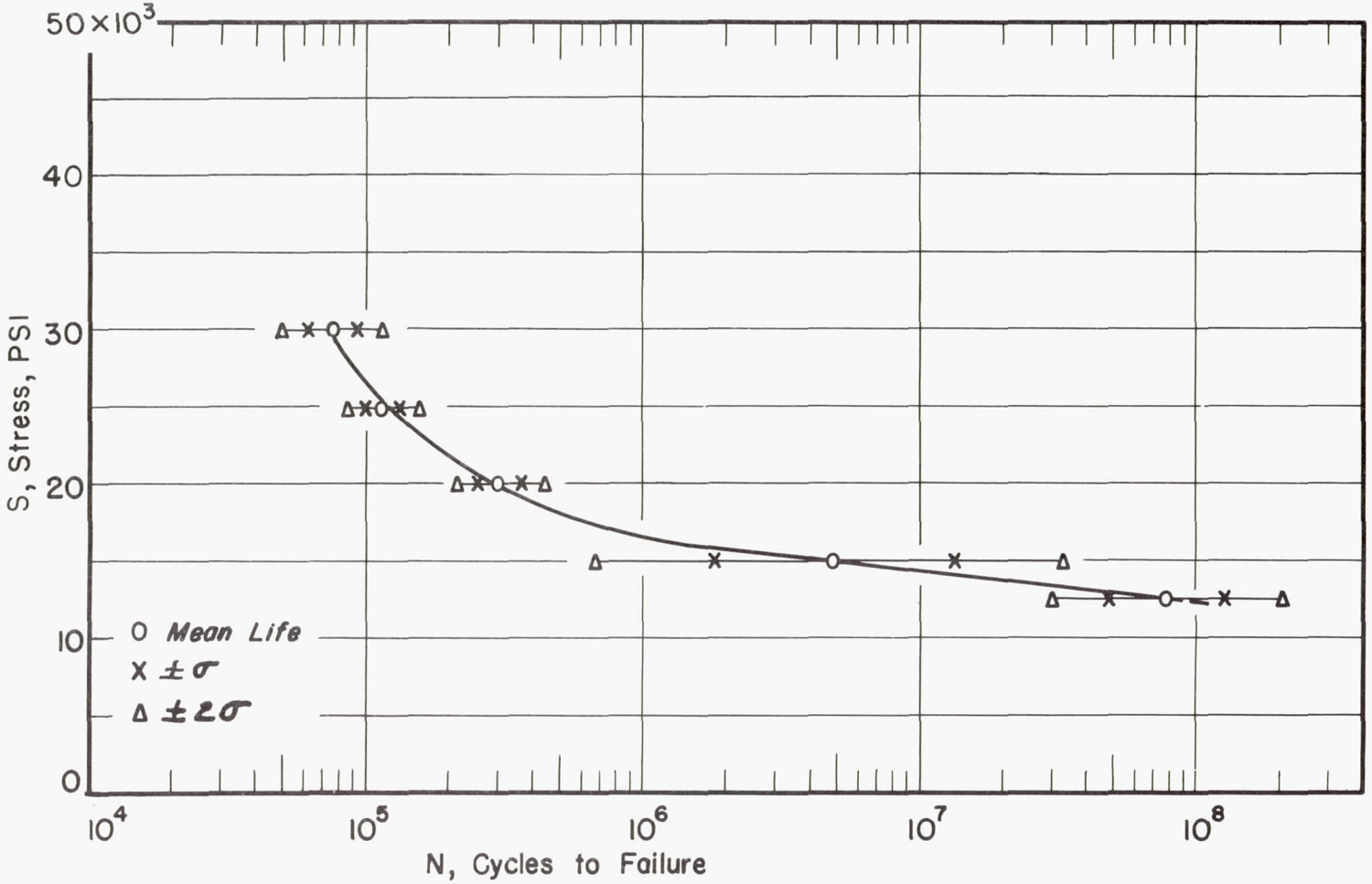
(b) Recrystallized.

Figure 6.- Etched macrostructures of extruded and extruded-plus-recrystallized longitudinal sections. Etched in Keller's etch; 1X.



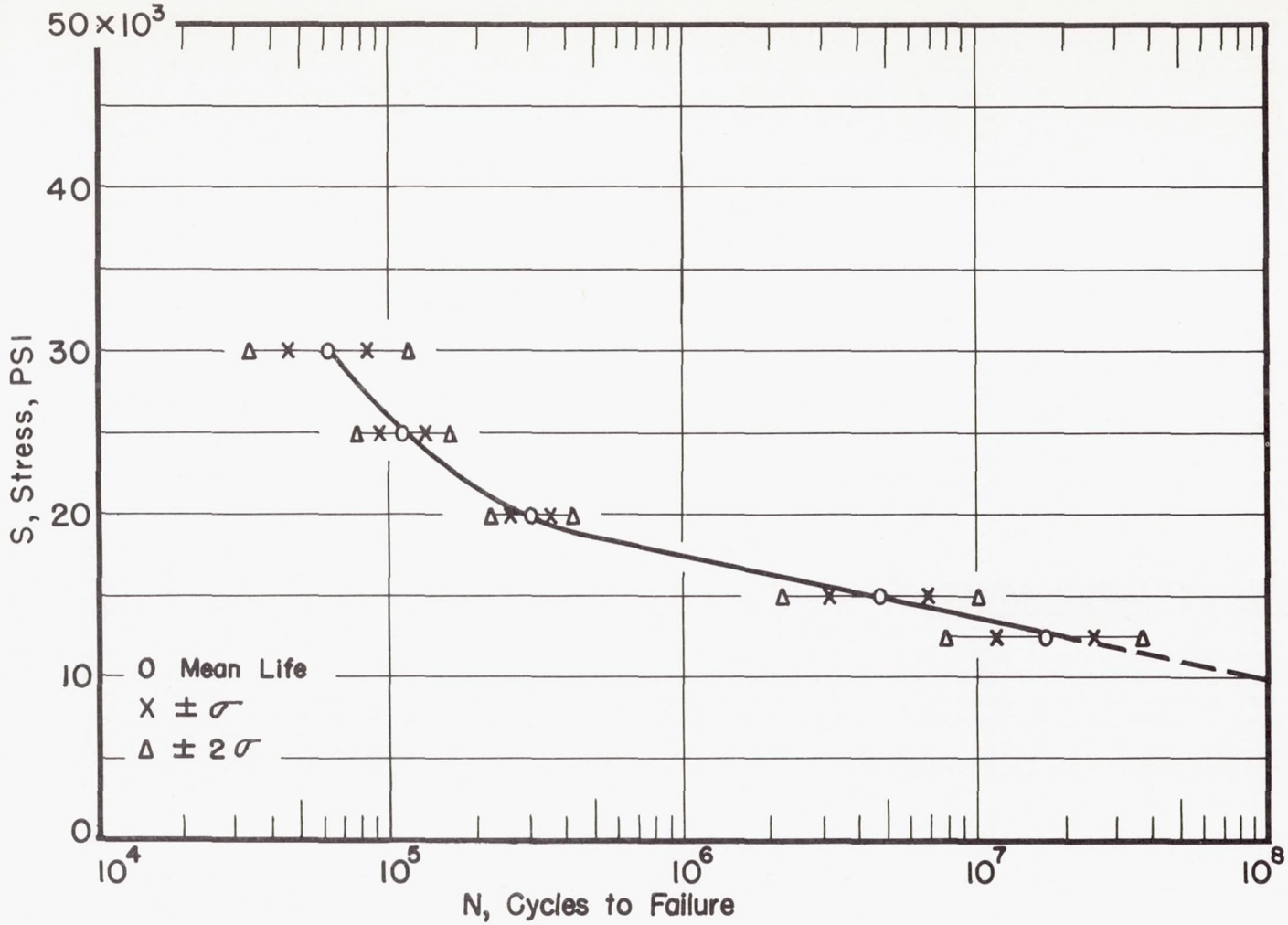
(a) Notched recrystallized transverse specimens.

Figure 7.- Statistical fatigue properties of longitudinal and transverse specimens of 24S-T4 aluminum alloy.



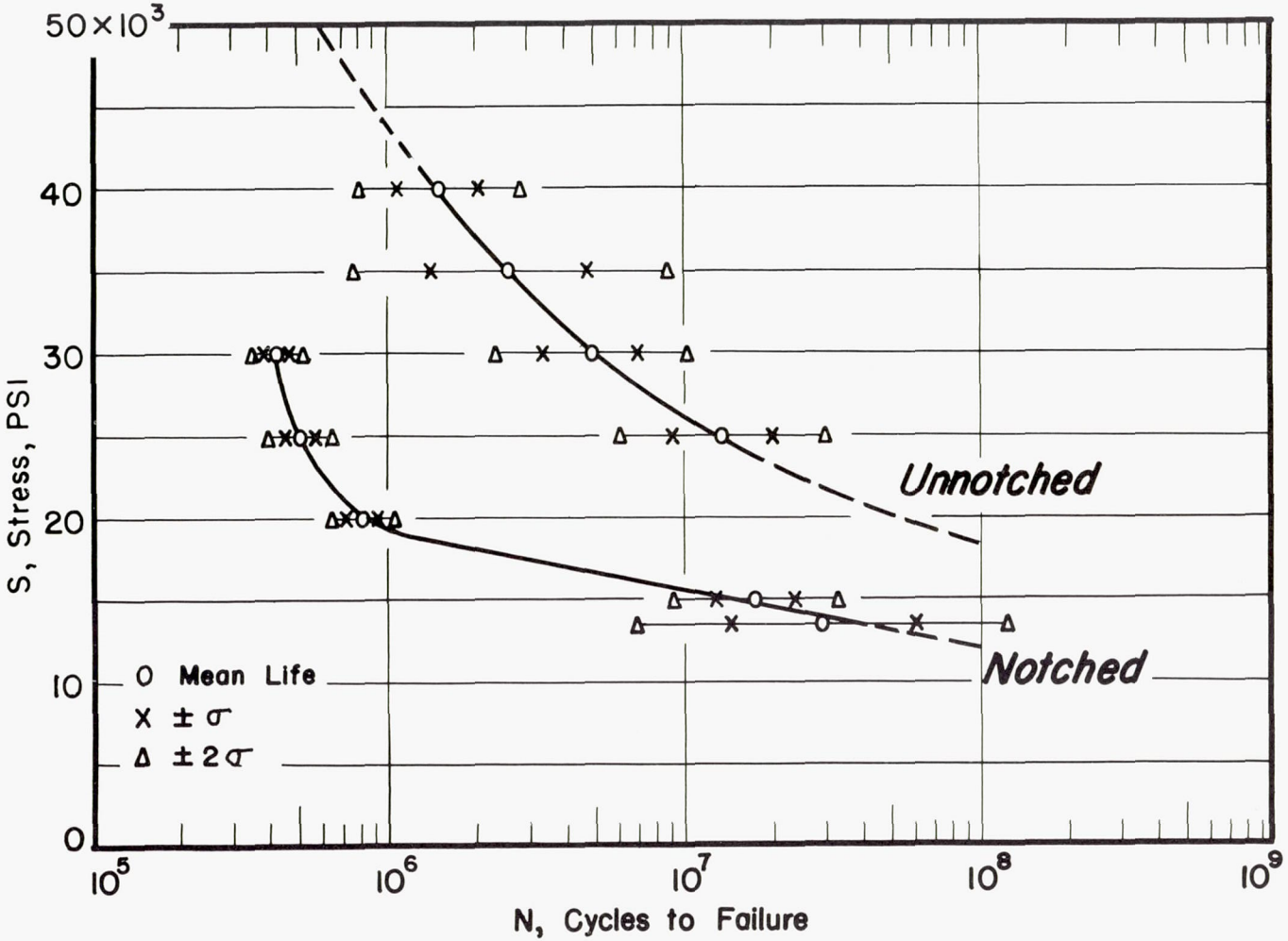
(b) Notched extruded transverse specimens.

Figure 7.- Continued.



(c) Notched recrystallized longitudinal specimens.

Figure 7.- Continued.



(d) Notched and unnotched extruded longitudinal specimens.

Figure 7.- Concluded.

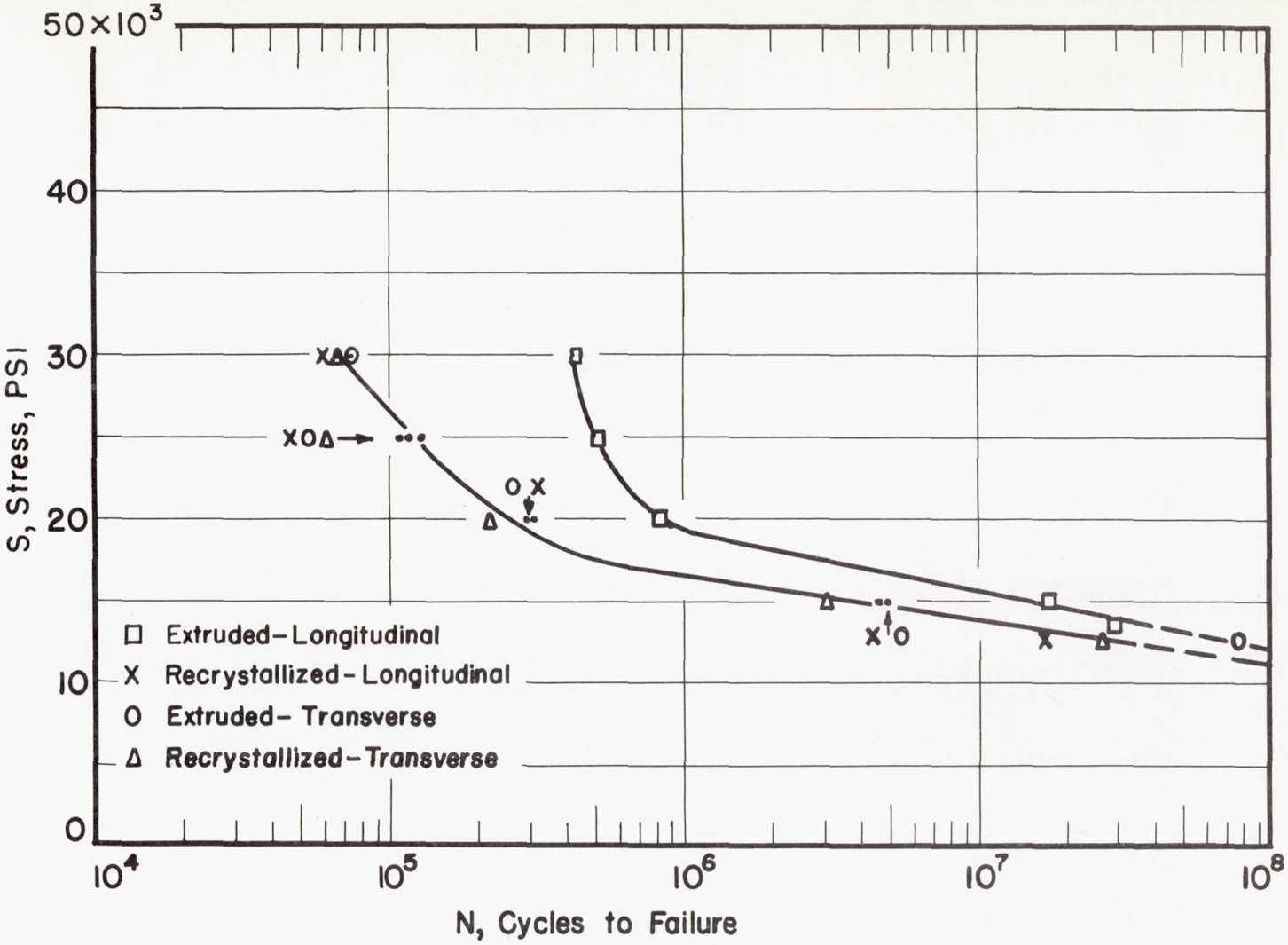
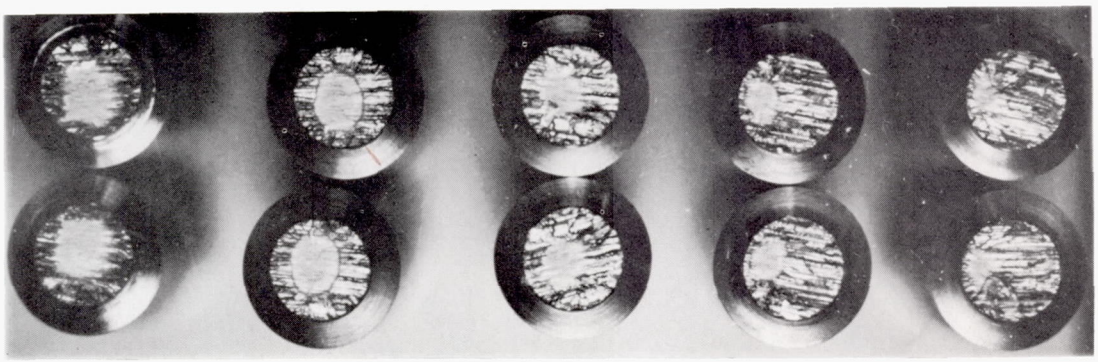
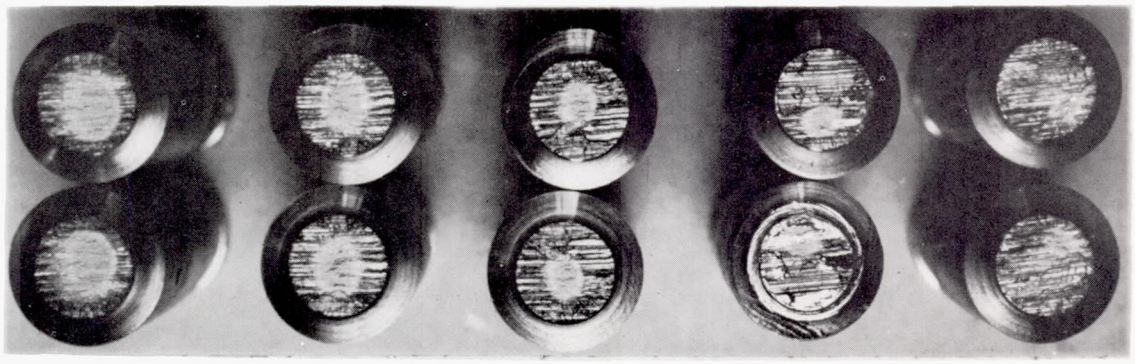


Figure 8.- Summary plot of mean fatigue properties of notched specimens of 24S-T4 aluminum alloy.



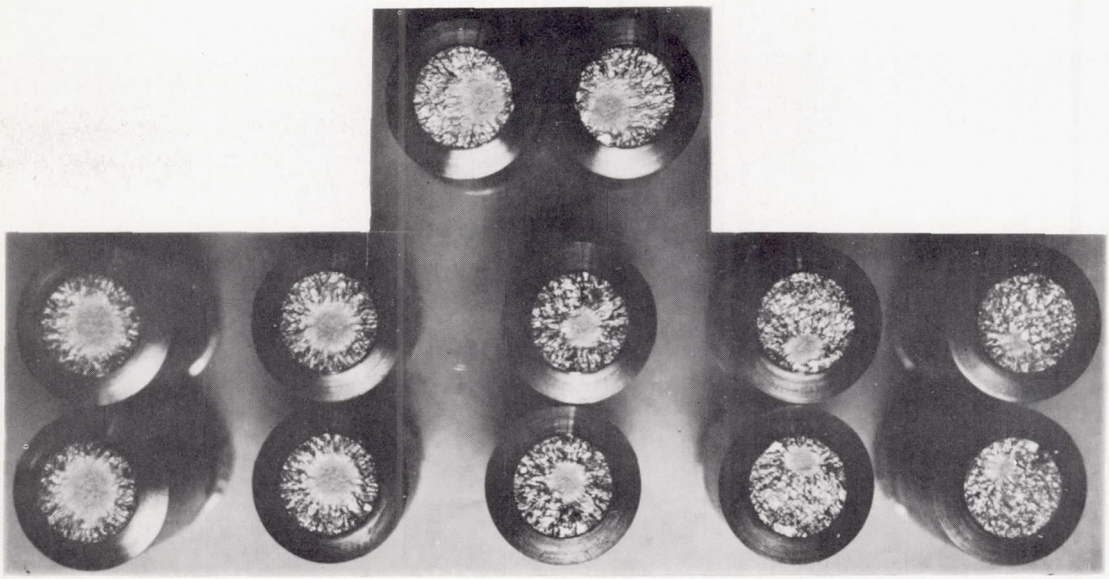
(a) Recrystallized. From left to right, at 30,000, 25,000, 20,000, 15,000, and 12,500 psi.



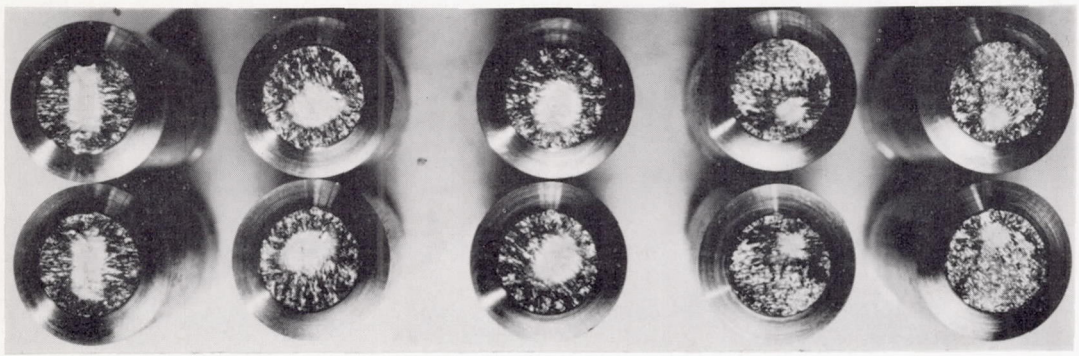
L-86060

(b) Extruded. From left to right, at 30,000, 25,000, 20,000, 15,000, and 12,500 psi.

Figure 9.- Fractures in transverse specimens. 2X.



(a) Recrystallized. Top, at 20,000 psi; bottom, from left to right, at 30,000, 25,000, 20,000, 15,000, and 12,500 psi.



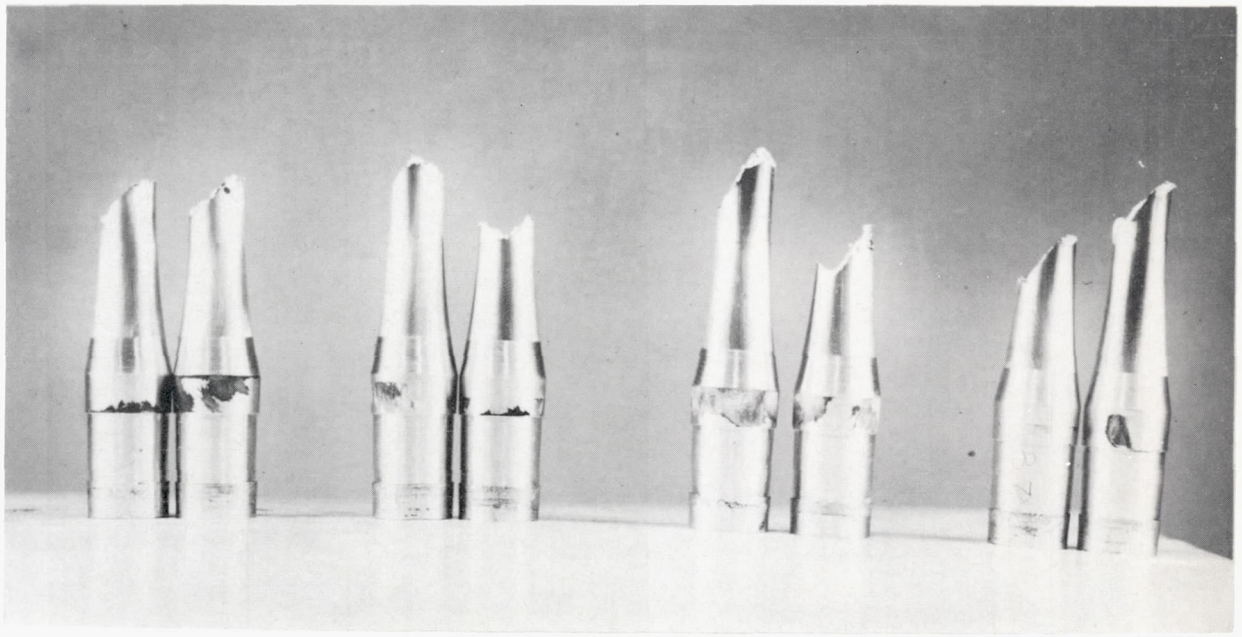
L-86061

(b) Extruded. From left to right, at 30,000, 25,000, 20,000, 15,000, and 13,500 psi.

Figure 10.- Fractures in longitudinal specimens. 2X.



(a) From left to right, at 35,000, 30,000, and 25,000 psi; 2X.



L-86462

(b) From left to right, at 40,000, 40,000, 30,000, and 30,000 psi; 1X.

Figure 11.- Fractures in unnotched extruded longitudinal specimens.

NACA-Langley - 3-14-55 - 1000